The effect of relative plasma plume delay on the properties of complex oxide films grown by multi-laser, multi-target combinatorial pulsed laser deposition

Katherine A. Sloyan[a*], Timothy C. May-Smith[a], Robert W. Eason[a], James G. Lunney[b]

(a) Optoelectronics Research Centre, University of Southampton, Highfield, Southampton, SO17 1BJ, UK

(b) School of Physics, Trinity College, Dublin 2, Ireland

Respective email addresses: kas@orc.soton.ac.uk, tcms@orc.soton.ac.uk, rwe@orc.soton.ac.uk, jlunney@tcd.ie

Abstract

We report the effects of relative time delay of plasma plumes on thin garnet crystal films fabricated by dual-beam, combinatorial pulsed laser deposition. Relative plume delay was found to affect both the lattice constant and elemental composition of mixed $Gd_3Ga_5O_{12}$ (GGG) and $Gd_3Sc_2Ga_3O_{12}$ (GSGG) films. Further analysis of the plasmas was undertaken using a Langmuir probe, which revealed that for relative plume delays shorter than ~200 μs, the second plume travels through a partial vacuum created by the first plume, leading to higher energy ion bombardment of the growing film. The resulting in-plane stresses are consistent with the transition to a higher value of lattice constant normal to the film plane that was observed around this delay value. At delays shorter than ~10 μs, plume propagation was found to overlap, leading to scattering of lighter ions from the plume and a change in stoichiometry of the resultant films.

* Corresponding author. Tel: +44 23 8059 3155, Email address: kas@orc.soton.ac.uk

Keywords

Pulsed laser deposition; thin film; garnet crystal; Langmuir probe; laser plasma, combinatorial

1. Introduction

Pulsed Laser Deposition (PLD) has proven to be a powerful and versatile tool in the fabrication of thin films. The high growth rate, simple experimental setup, lack of harmful precursor chemicals and fast changeover time compare favourably with many other fabrication techniques. A range of materials including polymers, metals and complex multicomponent oxides may be deposited, with functionalities and applications that include sensors, actuators and planar waveguides [1], among others.

Combinatorial PLD extends the basic PLD setup to include multiple lasers and targets, and currently shows great potential for precision materials engineering. Preliminary investigations have shown that the technique may be used to grow designer materials or alloys with deliberately engineered physical properties [2] and to enable greater control over film stoichiometry [3]. Notably, combinatorial PLD can also facilitate deposition of materials that cannot currently be fabricated via conventional, single laser, single target PLD. However, the inclusion of additional lasers and targets introduces a new set of parameters that must be optimised for efficient deposition and good quality films. One such parameter is the temporal coincidence (or otherwise) of the laser pulses, and, by extension, the synchronicity of the resulting plasma plumes.

Garnets are excellent laser host materials that in the past have been grown successfully via PLD by this group and others [4-7]. It has also been shown recently that two dissimilar garnets may be combined to yield a penternary single-crystal film [2]. The growth of films with specified, mixed compositions therefore presents the ideal scenario for selection and optimisation of various material parameters, such as refractive index, lattice constant and

thermal expansion coefficient, for applications in crystalline optical waveguide design and fabrication.

2. Experimental procedure

The setup for deposition was similar to that used previously by Gazia et al [2]. UV pulses (wavelength 266 nm) from two frequency quadrupled, flashlamp-pumped Nd:YAG lasers were incident upon rotating single-crystal garnet targets of $Gd_3Ga_5O_{12}$ (GGG) and doped (2 at. % Nd, 0.5 at. % Cr) $Gd_3Sc_2Ga_3O_{12}$ (GSGG) respectively. Pulse duration was nominally 5 ns and the laser repetition rate was 10 Hz. Films were deposited within a vacuum chamber with an ambient oxygen gas pressure of 4.2×10^{-2} mbar. The angle of incidence of the plumes onto the substrate was varied repeatedly over a range of 8°, in order to obtain a flat thickness profile. Laser fluence was approximately equal for both plumes, at values of ~1 J per cm^2, and target-substrate distance was ~50 mm for both targets.

Material from the two plasma plumes was deposited onto single crystal (100) orientated YAG substrates, of size 10×10×1 mm, producing epitaxial films of mixed GGG and GSGG. Films of pure GGG and GSGG were also grown on YAG substrates for comparison, using conventional single laser-single target deposition. A substrate temperature of ~650 $^{\circ}$C was maintained using a raster-scanned 10.6 μm wavelength CO_2 laser, and the substrate was rotated to aid uniform temperature film growth. Deposition time was 40 minutes for single crystal films and 20 minutes for mixed films, yielding films ~2.5 μm in thickness.

A Stanford DG535 digital delay generator was used to introduce a discrete delay between the two laser pulses for each of the films investigated, ranging from 3.2 μs to 50 ms. The laser flashlamps were triggered by the output signal from the DG535, with subsequent Q-switching and laser pulse output occurring around 180 μs later, according to each lasers' optimised internal settings. A difference in the optimised Q-switching time of the two lasers was measured using a photodiode and oscilloscope and was found to be 3.55 μs ± 0.05 μs.

Films were also grown with synchronised plumes. For this case, a single pulse was split from the DG535 and used to simultaneously trigger the flashlamps of both lasers. A second pulse was similarly used to trigger the Q-switch of each laser, synchronously to ±1 ns. The difference in path length (from laser to target surface) was measured as ~30 cm, corresponding to an additional relative delay of 1 ns. It should be noted that cable lengths, in both the synchronous and asynchronous cases, were equal, and hence should not account for any unintentional further error in delay measurements. It was also assumed for both lasers that error in laser response time (i.e. Q-switch to firing time) was negligible.

A Siemens D5000 X-ray diffractometer (XRD) was used to acquire diffraction spectra and a KLA Tencor P16 stylus profiler was used to measure film thickness. An Oxford Inca PentaFet-x3 electron dispersive x-ray analyser (EDX), connected to a Zeiss EVO-50 scanning electron microscope (SEM), was used to determine elemental composition.

Further analysis of the plasma plumes was carried out using a planar Langmuir probe [8], held in position in place of the substrate. The probe was biased at –30 V and measurements were taken across a 39 Ω load resistor, with two parallel 0.66 μF capacitors used to prevent charge saturation. The probe circuit (Koopman circuit) is shown in figure 1. Experiments were

conducted at the same deposition ambient oxygen pressure (4.2×10^{-2} mbar), and a constant plume-substrate angle of incidence of 23° was maintained. After around 2 minutes, the probe became coated with deposited oxide material that progressively and substantially reduced the measured signal strength. Measurements were therefore obtained in groups, each group taking no more than ~60 seconds, after which the probe was removed, cleaned and replaced.

3. Results and discussion

Figure 2 shows the variation in film lattice constant normal to the film plane with increasing plasma plume delay. Delay values here take into account the difference in Q-switching times between the two lasers. Two distinct regions of lattice constant (A and B) may be observed, with a transition region (C) occurring between ~150 μs and ~1 ms. Although the exact position of this transition region appears to vary slightly depending on plume order, the same overall trend is observed both in the case of the GGG plume arriving at the substrate first (followed by the GSGG plume) and vice versa. It should be noted that the lattice constant obtained using a delay of 100 ms (i.e. completely synchronous plumes) shows the same behaviour (within experimental error) as the lattice constant for a delay of 50 ms (i.e. completely asynchronous). All lattice constants were obtained via XRD analysis, with peaks normalised to the peak position of the underlying YAG substrate.

Figure 3 shows the variation in composition with increasing delay, as obtained via EDX measurements, irrespective of which plume arrived first at the substrate. Oxygen content may not accurately be measured via EDX, and hence was assumed to be stoichiometric for this analysis. Additional dopant concentrations were neglected, as the concentrations were too low

to be detected via EDX. Any significant trend corresponding to the change in lattice constant is not apparent, as composition does not appear to change significantly over most of the delay range. However, a small increase in Gd concentration, corresponding to a decreasing Sc concentration, may be observed for delays below approximately 13 μs.

Small variations in elemental composition were also observed across the surface of each film, due to the radial distribution of elements within the plumes. Random small fluctuations in O_2 pressure and laser power, as well as small variations in temperature due to differences in heat sinking, can be expected to lead to variation in crystal quality and lattice constant between different films at the same plume delay. The effects on lattice constant and composition of both these fluctuations and instrument errors were estimated using the standard error over multiple experiments, i.e. multiple films grown with the same delay. This analysis was carried out for delays of 3.63 μs and 100 μs (i.e. synchronous), and the results for lattice constant are illustrated on figure 2. Errors in composition were too small to be seen on figure 3.

Ion probe experiments were carried out with the GGG plume following the GSGG plume, the opposite plume order to the majority of the data presented in figure 2. Integrated ion flux was found to be only 1% of the deposited cations, and hence ion signals are not fully representative of the overall deposition flux; however, overall trends were observed and compared with lattice and composition data, with some approximate quantitative data obtained.

Figure 4 shows ion probe signals for both the GSGG and GGG plumes at background pressures of 4.2×10^{-2} mbar (a) and (b), and 1.2×10^{-5} mbar (i.e. vacuum) (c) and (d). In case (b), the signal shown represents the GGG plume only (i.e. no GSGG plume in the chamber),

to prevent the signal being disrupted by a previous plume. A sharp spike may be observed before the main pulse, labelled 'S' on figures 4(a) and 4(b). This serves as a zero time marker for measuring ion time-of-flight (TOF), and is due to electron emission from the probe caused by extreme ultraviolet emission of the ablation plasma during laser irradiation.

In vacuum, each signal shows a single peak, first rising rapidly to a maximum at a TOF of 4.4 μs after the ablation plasma front reaches the probe, then falling as the plume front expands beyond the probe. This TOF gives an ion velocity of 1.1×10^{4} ms^{-1}, which for gallium corresponds to an ion energy of 44 eV.

In an oxygen environment, the ion signal has two peaks: a somewhat attenuated peak around the same TOF as the vacuum case and a second peak around 10 μs. This so-called 'plume splitting' is a well-known feature of propagation of laser ablation plumes in a low pressure gas [9-10]. It arises in the pressure regime where some plume ions arrive at the probe without collision with the gas, while the remainder collide with the gas and propagate within a blast wave which arrives at a later time. The TOF of the second peak cannot be used directly to find the ion velocity, as the blast wave is continuously decelerated by the pressure and inertia of the gas. Looking at the attenuation of the first peak, and noting that the density of oxygen molecules at this pressure is 1.1×10^{15} cm^{-3}, we estimate that the ion-molecule scattering cross-section is 1.6×10^{-16} cm^{-2}, which is comparable to values found elsewhere [10].

Of primary interest is the change in propagation of the second plume as a function of delay between first and second laser plumes. Figure 5(a) shows the ion signal for both plumes for a time delay of 16 μs and Figures 5 (b-e) show signals for the second plume only at time delays of 40, 200, 400 and 1600 μs respectively. For a 16 μs delay, the two ion signals are partially

overlapped and are similar to the addition of the signals from single plumes in gas. At 40 μs delay (figure 5(b)), the signal for the second plume is similar, but is now separate from the first plume signal. At a 200 μs delay, however, the signal for the second plume has changed: the first peak is less attenuated and the second peak is relatively weaker, appearing as though, in this delay regime, the second plume is propagating in a lower gas pressure. This effect, i.e. partial vacuum generation by the first plume sweeping away gas in front of the target-probe region, has been observed before at higher gas pressure [11]. For delays beyond ~400 μs, the ion signal of the second plume is again very similar to that of the plume on its own in gas. It would appear, therefore, that for long delays the partial vacuum created by the first plume is refilled by gas flow before the second plume arrives.

It can be expected that the time scale for this refilling will be determined by the size of the refilled region and the sound velocity in the gas. Since the two ablation plumes are not collinear, details of the overall gas dynamical interaction of the plumes are complicated. However, taking the target-probe distance as an estimate of the region of partial vacuum, we can expect that it will be refilled in about 170 μs; this is consistent with the delay beyond which the ion signal of the second plume becomes gas-like again.

These features of ablation plume propagation may also provide an insight into a possible mechanism governing the observed compositional changes. For delays less than ~10 μs, the arrival of the two ablation plumes at the substrate is partially overlapped in time. It is not clear why this overlap should cause these compositional changes; it may be that the plumes are forcing a certain amount of gas into the region near the substrate, and the lightest of the cations are preferentially scattered sideways.

The small decrease in lattice constant for delays beyond ~200 μs coincides with the change of plume 2 ion signal from more vacuum-like to more gas-like. Ion energies associated with the earlier feature in both plumes are sufficient to cause sputtering [12]; however, we do not see any change in film composition, which would be associated with the preferential sputtering of one cation species. Ion bombardment of the growing film can cause in-plane compressive stress, which will be evidenced by a higher value of lattice constant normal to the film plane [13]. The higher value of lattice constant for delays below ~200 μs may therefore be due to higher energy ion bombardment of the growing film. For delays greater than 200 μs, the partial vacuum created by the first plume will be refilled and collisions with oxygen will slow down a significant fraction of the ions in the second plume.

In the broader context of determining optimum plume delay for multi-beam PLD geometries, we can therefore present two conclusions. Firstly, delay should be sufficiently long as to avoid plume-plume interaction near the substrate, and secondly, when a gaseous atmosphere is used, the delay of the following plume should be long enough to allow refilling of any partial vacuum created by the propagation of the earlier plume. A delay greater than ~1 ms is, for example, appropriate for the geometry and materials used in this experiment.

4. Conclusion

It has been shown that the lattice constant and composition of thin garnet films fabricated by dual-beam, combinatorial PLD depend on the relative delay between plasma plumes. Ion signal analysis, using a Langmuir probe technique, suggested that at delays less than ~200 μs, the second plume travels through a partial vacuum created by the first plume, leading to

higher energy ion bombardment of the growing film and increased in-plane compressive strain. These were observed as a change in lattice constant. Also, plume propagation will overlap at delays of less than ~10 μs, causing scattering of lighter cations from the plumes and leading to a change in elemental composition of the film grown. These results suggest a broad principle for the design of multi-beam PLD: plasma plume delay should be sufficiently long both to avoid plume overlap and to allow refilling of any partial vacuum created by an earlier plume.

Acknowledgements

This work was funded by the Engineering and Physical Sciences Research Council (EPSRC) under grant no. EP/F019300/1. The authors wish to acknowledge the services of the EPSRC National Crystallography Service, based at the School of Chemistry, University of Southampton. K. A. Sloyan would like to acknowledge the support of an EPSRC studentship.

References

[1] R.W. Eason (ed.), Pulsed Laser Deposition of Thin Films: Applications-Led Growth of Functional Materials, Wiley, New Jersey, 2007.

[2] R. Gazia, T.C. May-Smith, R.W. Eason, Growth of a hybrid garnet crystal multilayer structure by combinatorial pulsed laser deposition, Journal of Crystal Growth 310 (2008) 3848-3853.

[3] M.S.B Darby, T.C. May-Smith, R.W. Eason, Deposition and stoichiometry control of Nd-doped gadolinium gallium garnet thin films by combinatorial pulsed laser deposition using two targets of Nd:$Gd_3Ga_5O_{12}$ and Ga_2O_3, Appl. Phys. A. 93 (2008) 447-481.

[4] J. Gottmann, D. Wortmann, I. Vasilief, L. Moiseev, D. Ganser, Manufacturing of Nd:$Gd_3Ga_5O_{12}$ ridge waveguide lasers by pulsed laser deposition and ultrafast laser micromachining, Appl. Surf. Sci. 254 (2007) 1105-1110.

[5] T.C. May-Smith, R.W. Eason, Comparative growth study of garnet crystal films fabricated by pulsed laser deposition, Journal of Crystal Growth 308 (2007) 382-391.

[6] T.C. May-Smith, C. Grivas, D.P. Shepherd, R.W. Eason, M.J.F. Healy, Thick film growth of high optical quality low loss (0.1 dB cm^{-1}) Nd:$Gd_3Ga_5O_{12}$ on $Y_3Al_5O_{12}$ by pulsed laser deposition, Appl. Surf. Sci 223 (2004) 361-371.

[7] C. Grivas, T.C. May-Smith, D. Shepherd, R.W. Eason, Laser operation of a low loss (0.1 dB/cm) Nd:$Gd_3Ga_5O_{12}$ thick (40 μm) planar waveguide grown by pulsed laser deposition, Optics Communications 229 (2004) 355-361.

[8] B. Doggett, J.G. Lunney, Langmuir probe characterization of laser ablation plasmas, J. Appl. Phys. 105 (2009) 033306.

[9] R. F. Wood, J. N. Leboeuf, D. B. Geohegan, A. A. Puretzky, K. R. Chen, Dynamics of plume propagation and splitting during pulsed-laser ablation of Si in He and Ar, Phys. Rev. B. 58 (1998) 1533-1543.

[10] S. Amoruso, J. Schou, J. G. Lunney, Multiple-scattering effects in laser ablation plume propagation in gases, Europhys. Lett. 76 (2006) 436-442.

[11] L. Peter, R. Noll, Material ablation and plasma state for single and collinear double pulses interacting with iron samples at ambient gas pressures below 1 bar, Appl. Phys. B 86 (2007) 159-167.

[12] L.S. Dorneles, D. O'Mahony, C.B. Fitzgerald, F. McGee, M. Venkatesan, I. Stanca , J.G. Lunney, J.M.D. Coey, Structural and compositional analysis of transition-metal-doped ZnO and GaN PLD thin films, Appl. Surf. Sci. 248 (2005) 406-410.

[13] D. P. Norton, Synthesis and properties of epitaxial electronic oxide thin-film materials Mater. Sci. Eng. R. 43 (2004) 139-247.

Figure captions

[Figure 1]: Koopman circuit used in Langmuir ion probe experiments

[Figure 2]: Graph of film lattice constant for different plume delay values, as obtained via XRD analysis. Data for both plume arrival orders (GGG plume first, GSGG plume first) have been included. Regions of higher lattice constant (around 12.49Å) and lower lattice constant (around 12.46Å) may be observed (labelled A and B respectively), along with a transition region (C) between ~150 μs and ~1 ms.

[Figure 3]: Graph of film elemental composition for different plume delay values, including data from both plume arrival orders (GGG plume first, GSGG plume first). Above ~13 μs there does not appear to be a significant trend in compositional variation, although a small Sc decrease and corresponding Gd increase may be observed below ~13 μs.

[Figure 4]: Ion probe signals for plumes 1 and 2 (a) GSGG plume signal, (b) GGG plume signal, both at background pressure of 4.2×10^{-2} mbar. Spike serving as zero time marker labelled as 'S'. (c) GSGG plume signal, (d) GGG plume signal, both in vacuum (background pressure = 1.2×10^{-5} mbar).

[Figure 5]: Examples of plume 2 ion probe signals for various delays: (a) signal for delay of 16 μs (both plumes), (b) delay of 40 μs (c) delay of 200 μs (d) delay of 400 μs (e) delay of 1600 μs. Time axis 0 taken as moment of production of plume 2.

Figure(s)

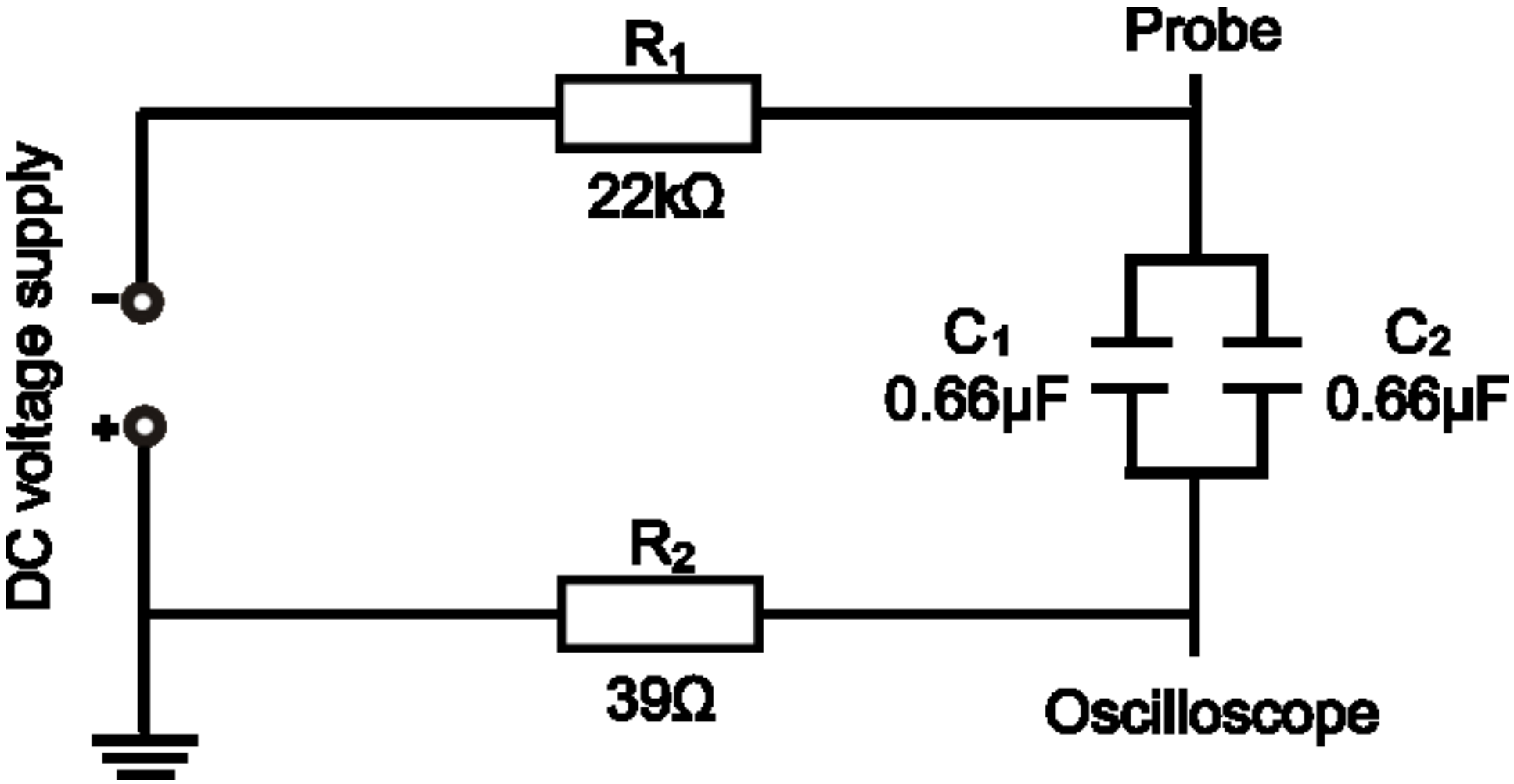
R1
Probe
22kΩ
DC voltage supply
-
+
C1
0.66μF
C2
0.66μF
R2
39Ω
Oscilloscope

Figure(s)

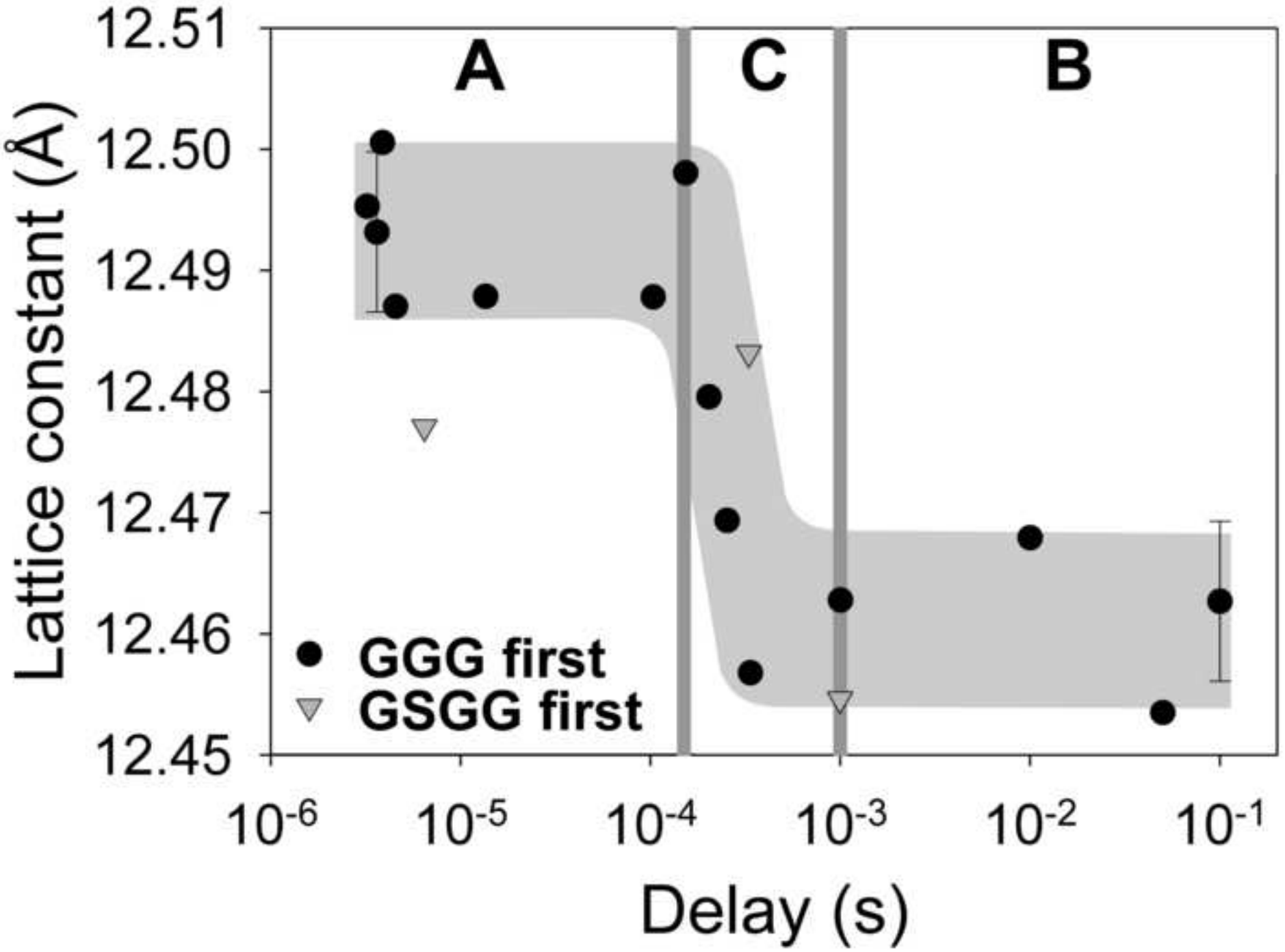
12.51
12.50
12.49
12.48
12.47
12.46
12.45
Lattice constant (Å)
A
C
B
GGG first
GSGG first
10-6
10-5
10-4
10-3
10-2
10-1
Delay (s)

Figure(s)

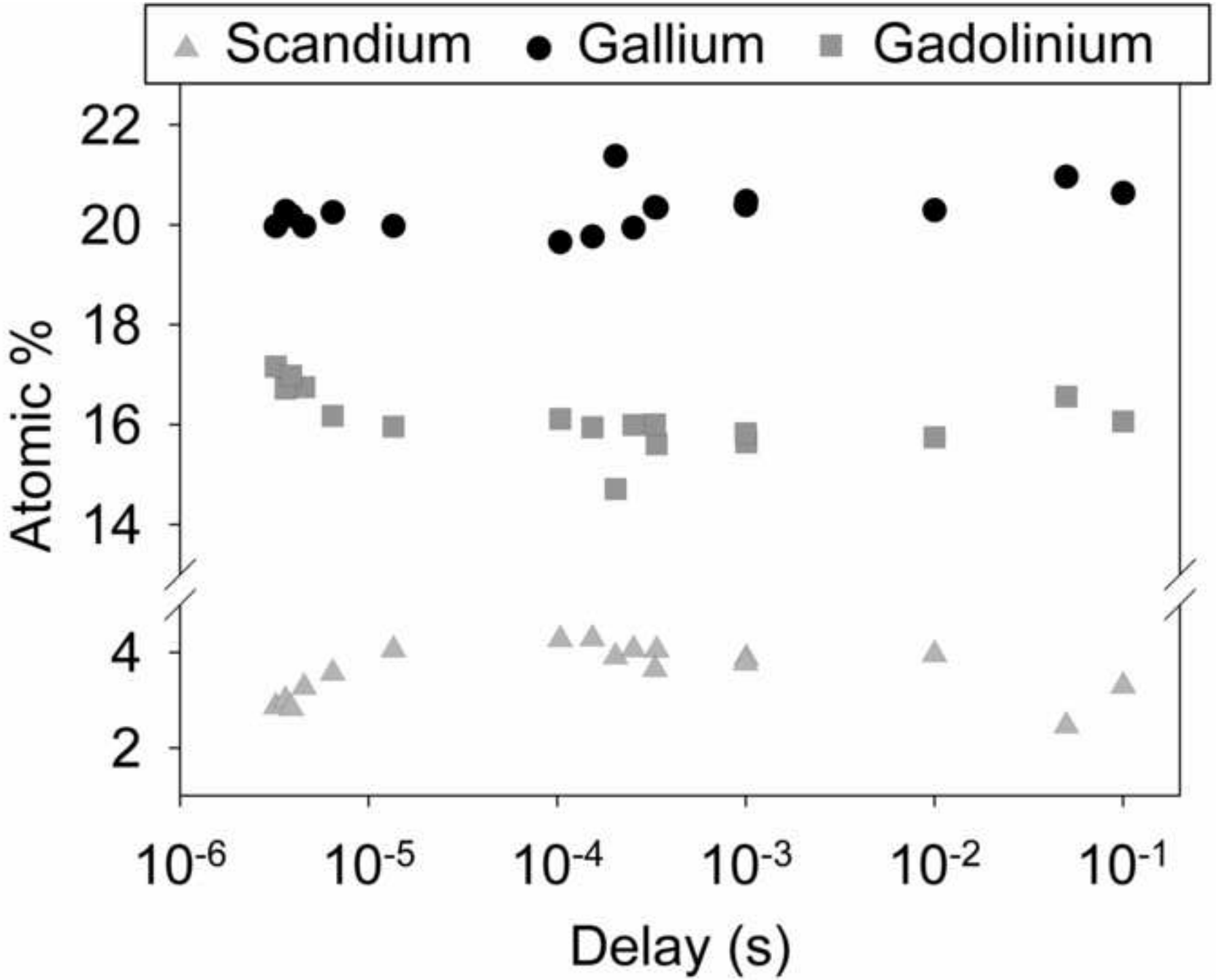
Scandium
Gallium
Gadolinium
Atomic %
22
20
18
16
14
4
2
10-6
10-5
10-4
10-3
10-2
10-1
Delay (s)

Figure(s)

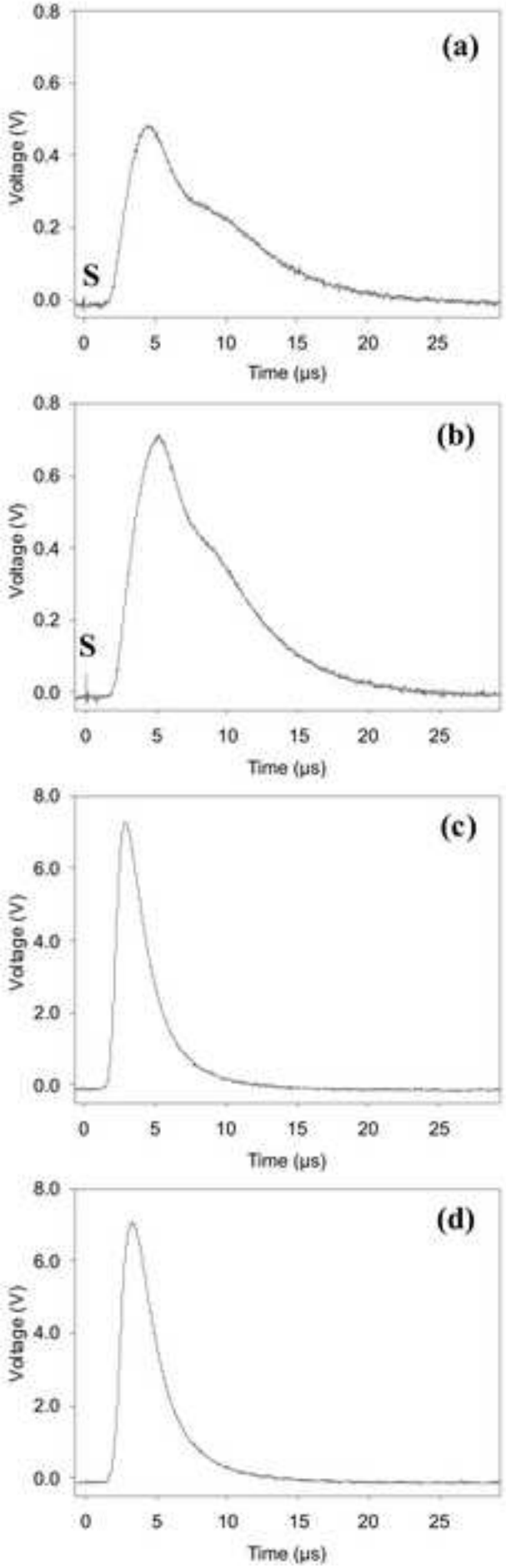
(a)
Voltage (V)
0.8
0.6
0.4
0.2
0.0
S
0
5
10
15
20
25
Time (μs)
(b)
Voltage (V)
0.8
0.6
0.4
0.2
0.0
S
0
5
10
15
20
25
Time (μs)
(c)
Voltage (V)
8.0
6.0
4.0
2.0
0.0
0
5
10
15
20
25
Time (μs)
(d)
Voltage (V)
8.0
6.0
4.0
2.0
0.0
0
5
10
15
20
25
Time (μs)

Figure(s)